

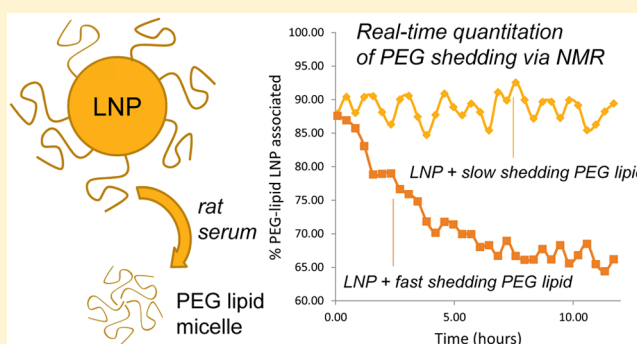
Real Time Measurement of PEG Shedding from Lipid Nanoparticles in Serum via NMR Spectroscopy

Stephen C. Wilson, Jeremy L. Baryza, Aimee J. Reynolds, Keith Bowman, Mark E. Keegan, Stephany M. Standley, Noah P. Gardner, Parul Parmar, Vahide Ozlem Agir, Sunita Yadav, Adnan Zunic, Chandra Vargeese, Cameron C. Lee,* and Srinivasan Rajan*

Novartis Institutes for Biomedical Research, 250 Massachusetts Avenue, Cambridge, Massachusetts 02139, United States

ABSTRACT: Small interfering RNA (siRNA) is a novel therapeutic modality that benefits from nanoparticle mediated delivery. The most clinically advanced siRNA-containing nanoparticles are polymer-coated supramolecular assemblies of siRNA and lipids (lipid nanoparticles or LNPs), which protect the siRNA from nucleases, modulate pharmacokinetics of the siRNA, and enable selective delivery of siRNA to target cells. Understanding the mechanisms of assembly and delivery of such systems is complicated by the complexity of the dynamic supramolecular assembly as well as by its subsequent interactions with the biological milieu. We have developed an ex vivo method that provides insight into how LNPs behave when contacted with biological fluids. Pulsed gradient spin echo (PGSE) NMR was used to directly measure the kinetics of poly(ethylene) glycol (PEG) shedding from siRNA encapsulated LNPs in rat serum. The method represents a molecularly specific, real-time, quantitative, and label-free way to monitor the behavior of a nanoparticle surface coating. We believe that this method has broad implications in gaining mechanistic insights into how nanoparticle-based drug delivery vehicles behave in biofluids and is versatile enough to be applied to a diversity of systems.

KEYWORDS: PGSE NMR, LNP, lipid nanoparticle, nanoparticle, liposome, micelle, PEG shedding, PEG-lipid, siRNA



INTRODUCTION

Small interfering RNA (siRNA) based therapeutics have the potential to provide new routes of treatment for diseases ranging from cancer¹ to rare genetic diseases.² Since unprotected siRNA is unstable to nucleases, is rapidly excreted via the kidneys, and is membrane impermeable, effectively delivering siRNA to the cytosol of cells remains the most significant roadblock preventing their medical use. To become relevant medicines, siRNA-based therapeutics demand the development of well-tolerated delivery systems that enable their transport and uptake by target cells.³

Thanks to the pioneering work of Cullis, MacLachlan, and others,⁴ lipid nanoparticles (LNPs)—multicomponent cationic lipid nanoparticles containing siRNA—are among the leading technologies, if not the leading technology, in the race to achieve an effective delivery system for siRNA-based therapies. Highly potent and effective delivery of siRNA by LNPs has been demonstrated in preclinical studies involving the liver and solid tumors, and LNP mediated delivery of siRNA is currently undergoing clinical evaluation in several trials.^{2,5,6} One key to the development of tissue specific LNP-mediated delivery of siRNA has been the recognition that the nature of the hydrophilic “steric-stabilizing” lipids strongly influences the distribution and tissue disposition of the particles. The most commonly employed steric stabilizer, poly(ethylene glycol)

(PEG), is thought to act as a protective coating material around the nanoparticle, opposing deleterious interactions with various biomolecules encountered in vivo and preventing the nanoparticle from clearance by the reticuloendothelial system (RES).⁷ Typically, the PEG is anchored to the lipid nanoparticle by attaching a lipophilic tail to one end of the polymer. The tail embeds itself into the lipid membrane, leaving the PEG with more mobility on the surface of the lipid nanoparticle. Stabilized lipid nanoparticles result in a longer blood circulation half-life and greater exposure to multiple cell types. While RES avoidance allows LNPs increased access to nonphagocytic cells in the bloodstream, it is thought to be undesirable for the PEG-lipid coating to remain once the nanoparticle reaches its target cells. Steric stabilizers reduce the interaction of the particle with the target cells, thereby reducing cellular uptake and cytosolic delivery. To achieve effective delivery, it is believed that some or all of the PEG-lipid coating

Special Issue: Next Generation Gene Delivery Approaches: Recent Progress and Hurdles

Received: June 3, 2014

Revised: December 29, 2014

Accepted: January 3, 2015

Published: January 12, 2015

must be expelled from the particle surface prior to cellular uptake. The loss of the steric shielding around the LNP is herein referred to as “PEG shedding”. The timing of PEG shedding is an important feature of an effective LNP: shed too quickly, and LNP biodistribution is primarily limited to the liver; shed too slowly, and though LNP distribution to extrahepatic tissues becomes possible, intracellular internalization of the LNP may be hindered.⁷ In effect, understanding the role of PEG shedding is crucial to the mechanistic understanding and development of siRNA-based therapeutics.

There is a clear need for analytical methods capable of measuring PEG shedding, for it would allow mechanistic insight into the phenomenon, would provide a screening tool for studying the interaction of nanoparticles in diverse biological settings, and could potentially reduce experimental animal consumption. Until recently, PEG shedding from lipid nanoparticles had never been directly observed. Instead, PEG shedding had been inferred indirectly using lipid exchange⁸ or functional *in vitro* or *in vivo*⁹ assays. Recently, PEG shedding from nanoparticles in biofluids was confirmed by chromatographic separation of particle-bound and shed PEG-lipid (with PEG-lipid quantified by radiolabeling¹⁰ or LC/MS–MS¹¹) and by monitoring the fluorescence of profluorescent PEGs that have quenched fluorescence prior to PEG shedding.¹² These powerful new methods have proven the existence of PEG shedding, but involve considerable sample handling and/or require fluorescent labeling of the PEG, which makes the process of monitoring PEG nonconductive to real-time measurement and carries the risk that the label on the PEG or the separation process influences the PEG shedding behavior.

Pulsed gradient spin echo (PGSE) NMR is a powerful technique for studying translational motion.^{13,14} Because of the precedent in using PGSE NMR to study the diffusion of drug delivery systems,¹⁵ we hypothesized that the technique would have utility in the analysis of PEG shedding kinetics under simulated physiological conditions.¹⁶ Since PEG associated with a lipid nanoparticle diffuses much more slowly than free PEG, we are able to use PGSE NMR to measure the relative populations of the two over time, thereby obtaining a PEG shedding rate profile. The ability of ¹H NMR to distinguish between analytes based on their unique chemical shifts allows for molecularly specific interrogation of the system (in this instance the focus is on PEG). Herein, we describe a straightforward, quantitative, label-free, and real-time method that allows for the first time a direct measure of PEG shedding under *ex vivo* conditions using a conventional NMR setup with a high resolution probe. Furthermore, we believe that the general methods used have applicability beyond the world of lipid mediated siRNA delivery and could be used for NMR-based studies of a wide range of nanoparticle systems in biofluids.

RESULTS

Principles of the Method. Self-diffusion is defined as the stochastic motion of molecules at thermal equilibrium in a pure liquid.¹⁷ For evaluating our methodology, the self-diffusion of four previously described^{1,18} PEGylated LNPs in phosphate buffered saline (PBS) was measured using dynamic light scattering (DLS) and ¹H PGSE NMR. Subsequently, rat serum was added to the formulations, and ¹H PGSE NMR was used to quantify the rate of PEG shedding and qualify the supra-molecular structure of the detached PEG-lipid.

PEGylated lipid nanoparticles often display a strong, sharp PEG signal between 3.5 and 4.0 ppm in their ¹H NMR spectrum. This is due to the PEG's large number of repeating units and surface location. On the other hand, the ¹H NMR spectrum of rat serum is devoid of any intense peaks relative to the PEG resonance in this region. Broad peaks associated with endogenous proteins show up here but are almost completely removed under PGSE conditions as shown in Figure 1.¹⁹

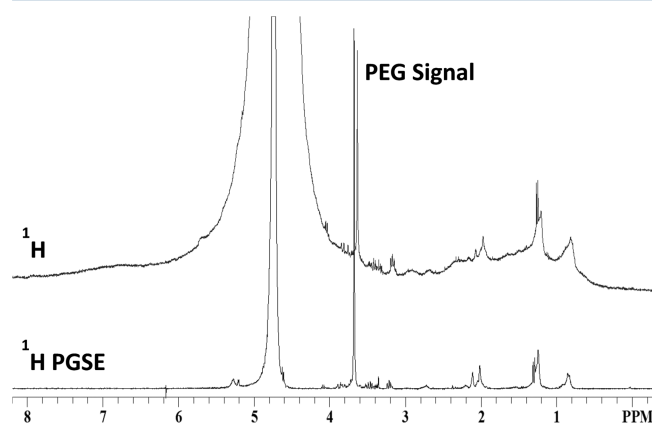


Figure 1. ¹H and ¹H PGSE spectrum of oleyl-C14 in rat serum. Broad resonances are filtered out and the water signal is greatly attenuated under PGSE conditions. A 7% gradient was applied for the ¹H PGSE spectrum. All other parameters are specified in Methods.

Application of the PGSE sequence effectively filters out components with fast T_2 relaxation (i.e., serum proteins) as well as attenuates resonances associated with quickly diffusing species (e.g., water), making the spectrum easier to analyze. These characteristics allow PEGylated lipid nanoparticles to be distinguished from the medium and make the study of PEG shedding in serum possible. Importantly, the method requires minimal handling: once mixed in an NMR tube, LNP and serum are placed in the spectrometer and ¹H PGSE NMR spectra can be acquired as often as desired without any further sample manipulation.

For interpretation of the results, we make the assumption that there is only PEG-lipid associated with the lipid nanoparticle and “free” PEG-lipid. The population associated with the lipid nanoparticle diffuses more slowly and is defined as having a diffusion coefficient consistent with that calculated from DLS measurements. Disparities between the two measurement techniques could be attributed to error in fit, differences between mediums (i.e., serum vs water), or the increased sensitivity of DLS toward species with larger dimensions in polydisperse samples. The free PEG-lipid population diffuses faster and may represent multiple species, since free PEG-lipid behaves as a surfactant in aqueous solution and can form micelles.²⁰ The CMCs of similar PEG-lipids in buffer have been reported by others to be on the order of 1–10 μ M,²¹ which is 20–200-fold lower than our experimental PEG-lipid concentrations. If the CMCs of PEG-C-DMA and PEG-C-DMA are on the higher end of the above range, it could be possible that a large enough unimer population exists in solution to affect the average diffusion coefficient measured by ¹H PGSE NMR. PEG-lipids can also associate with lipoprotein particles, which have micelle-like dimensions. Whether the PEG-lipid exists in unimer, micelle-associated, LNP-associated, or lipoprotein particle-associated states will depend on the

matrix and conditions in which the LNP exists. Whether the different states are resolved by the PGSE method depends on whether the exchange rates between the different states are slow on the NMR time scale. We define species with diffusion coefficient between $\sim 1 \times 10^{-10} \text{ m}^2/\text{s}$ (unimer) and $\sim 3 \times 10^{-11} \text{ m}^2/\text{s}$ (micelle) as free PEG-lipid, where the former value was extrapolated from the literature²² and the latter was experimentally determined in D_2O . Values obtained between the two extremes we interpret as weighted averages between the two states. Such a weighted average signifies fast exchange between the unimer and micellar states relative to the diffusion time of the PGSE experiment (197 ms).²³ Fast exchange between two species relative to the NMR diffusion time results in a single echo decay, whereas slow exchange results in an echo decay that can be described by a sum of exponentials, where each exponential is attributed to species with unique diffusion coefficients. In the fitting of our data we used an unbiased approach, choosing to use the fewest exponentials necessary to give a high quality fit. In all of the cases reported herein, monoexponential or biexponential fits were sufficient, though we have found it necessary to use a triexponential fit for certain circumstances (data not shown).

We demonstrate the necessity of a biexponential fit in Figure 2, in which an LNP was analyzed $\sim 12 \text{ h}$ after dilution into rat

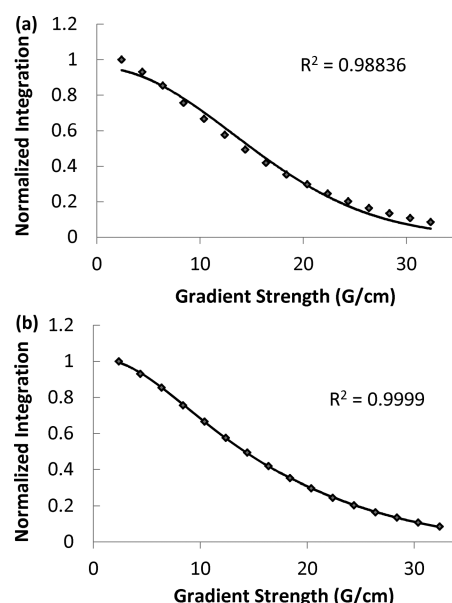


Figure 2. (a) PGSE decay of oleyl-C14/serum $\sim 12 \text{ h}$ after mixing (single exponential fit). (b) PGSE decay of oleyl-C14/serum $\sim 12 \text{ h}$ after mixing (double exponential fit).

serum. A single exponential fit exhibits large residuals and is a poor fit overall (Figure 2a). The poor quality of the single exponential fit is exacerbated as time passes and more PEG

dissociates from the lipid nanoparticle. The double exponential fit remedies the poor quality and presumably more accurately describes the system (Figure 2b).

It is important to mention that relative quantification of the two populations is dependent on the PEG's T_1 and T_2 relaxation being similar for all of its states (i.e., surface of the lipid nanoparticle, micelle, and unimer). We believe that this is a fair assumption because the PEG is exposed to similar relaxation environments in all three states.¹⁷

Self-Diffusion of Lipid Nanoparticles. Four distinct formulations were prepared to study the effect of (1) PEG-lipid tail length and (2) cationic lipid saturation on PEG shedding. Similar formulations have been described previously.^{1,18} Table 1 details the four formulations used in this study. The structures of the corresponding cationic lipids and PEG-lipids for the four formulations are illustrated in Figure 3.

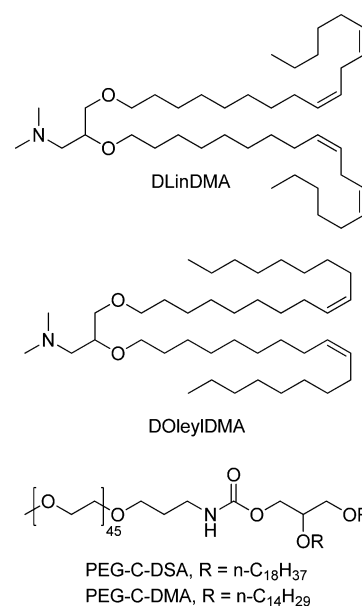


Figure 3. Cationic lipids and PEG-lipids employed for the study.^{9,18}

The self-diffusion coefficients derived from DLS measurements were back calculated using the Stokes–Einstein equation (eq 1), whereas those derived from NMR measurements were determined by fitting the PGSE decay curve with the single exponential Stejskal–Tanner equation (see Methods).

$$D = \frac{kT}{6\pi\eta R} \quad (1)$$

The discrepancy between the two values could be attributed to the increased sensitivity of the DLS measurement to species of larger dimensions in polydisperse samples (i.e., the LNP and adventitious larger particles relative to micelles or unimers) and/or to the NMR measurement being sensitive to the fast

Table 1. Formulation Details^a

formulation	cationic lipid	no. of double bonds in lipid tail	PEG	no. of carbons in lipid tail	d^{DLS} (nm)	$D^{\text{DLS}} \times 10^{12} \text{ (m}^2/\text{s)}$	$D^{\text{NMR}} \times 10^{12} \text{ (m}^2/\text{s)}$
linoleyl-C18	DLinDMA	4	C-DSA	18/18	73	7.0	13
linoleyl-C14	DLinDMA	4	C-DMA	14/14	82	6.3	16
oleyl-C14	DOleylDMA	2	C-DMA	14/14	73	7.1	17
oleyl-C18	DOleylDMA	2	C-DSA	18/18	74	6.9	16

^aAll measurements were performed at 300 K. Calculations used a water viscosity of $8.5 \times 10^{-4} \text{ Pa}\cdot\text{s}$.

on–off exchange of the PEG-lipid. The latter possibility refers to PEG-lipid molecules exchanging rapidly between the LNP-associated, micellar and unimer states, resulting in the diffusion coefficient measured by NMR being a weighted average of the lipid nanoparticle associated PEG-lipid population and the free PEG-lipid population. A study of PEGylated LNPs reported by Leal found that PEG-lipid exchange between the micellar and LNP states was slow when studied in buffer, but no comment on the exchange with the unimer population was made.²³ Since the decay curve we observe fits well with a single exponential, we conclude that either the exchange is fast relative to the diffusion time of the experiment (197 ms) or the micellar and unimer populations are very small. We believe that the DLS measurement represents a more accurate diffusion coefficient for the LNP because it is not focused on the PEG moiety and is more sensitive to the larger species (lipid nanoparticles) in the formulation.

Quantitation of PEG Shedding. Figure 4 illustrates the PEG shedding rate profiles for the four lipid formulations in rat

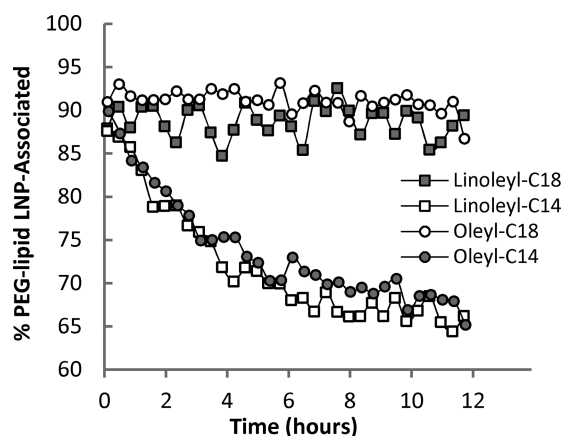


Figure 4. PEG shedding profiles for all formulations. Formulations with the shorter PEG-lipid shed more than those with the longer tail. The average absolute errors for the PEG-lipid LNP associated populations are as follows: linoleyl-C18 (1.0%), linoleyl-C14 (3.7%), oleyl-C14 (4.0%), and oleyl-C18 (0.7%).

serum. Upon the addition of serum, the initial fraction of LNP-associated PEG-lipid for all of the formulations at the first measurable time point was ~90%. This initial drop-off can be rationalized by one or both of two possible explanations. First, it is possible that the PEG-lipid sheds so rapidly between the time the formulation is mixed with serum and acquisition that data points within the first ~10% cannot be sampled. Another possibility is that ~10% of the PEG-lipid may already exist in the free PEG-lipid state in fast exchange with the lipid nanoparticle surface prior to the addition of serum, and that addition of serum to the formulation somehow slows the exchange kinetics between the various possible states the PEG-lipid can access (LNP, micelle, unimer). A slowed exchange would make observing and quantitating the proportion of PEG-lipid residing in each phase feasible. This explanation is consistent with the unexpectedly large self-diffusion coefficient found for the LNPs determined by NMR as follows: assuming that the free PEG-lipid has a diffusion coefficient of approximately $1 \times 10^{-10} \text{ m}^2/\text{s}$ and represents 10% of the total population, the calculated weighted average is $1.6 \times 10^{-11} \text{ m}^2/\text{s}$ and is in range with the experimentally determined NMR

self-diffusion coefficient values shown in Table 1 ($1.3\text{--}1.7 \times 10^{-11} \text{ m}^2/\text{s}$).

$$\begin{aligned} D &= p_F D_F + p_L D_L \\ &= 0.1 \times 1 \times 10^{-10} + 0.9 \times 7 \times 10^{-12} \\ &= 1.6 \times 10^{-11} \frac{\text{m}^2}{\text{s}} \end{aligned}$$

Here p_F is the fraction of the total PEG-lipid in the free PEG-lipid state, p_L is the fraction of the total PEG-lipid in the lipid nanoparticle state, D_F is the approximate diffusion coefficient for the free PEG-lipid, and D_L is the approximate diffusion coefficient for the LNP-bound PEG-lipid. While performing the same calculation using a more micelle-like value of $3 \times 10^{-11} \text{ m}^2/\text{s}$ does not produce a result as close to the experimentally determined value, it is also not completely unreasonable.

Linoleyl-C14 and oleyl-C14 shed ~35% of their PEG-lipid over the course of 12 h, whereas linoleyl-C18 and oleyl-C18 show no change over time. This indicates that those formulations with a smaller lipid tail shed faster than those with a longer tail. The PEG is covalently attached to a lipid anchor that embeds itself into the lipid nanoparticle's membrane. The hydrophobic forces between the lipid anchor and membrane are believed to fix the PEG-lipid to the lipid nanoparticle. By shortening the lipid chain, the surface area between the lipid and membrane is reduced, thereby diminishing the van der Waals forces holding the two together and allowing for more facile departure.²⁴ While the length of the PEG-lipid tail plays a large role in the extent of PEG shedding, varying the level of saturation present in the cationic lipid tails does not influence the rate of PEG loss significantly in this system.

Qualification of Translational Motion during PEG Shedding. The diffusion coefficients of the PEG-lipid populations also show distinction between those LNPs that shed and those that do not. Figure 5 describes the variation in diffusion coefficient values for the free PEG-lipid over time. For those LNPs that exhibit little shedding, the diffusion of the free PEG-lipid is consistent with a unimer below a critical micelle concentration (CMC) and remains fairly consistent over time. The erratic behavior of these values is attributed to the

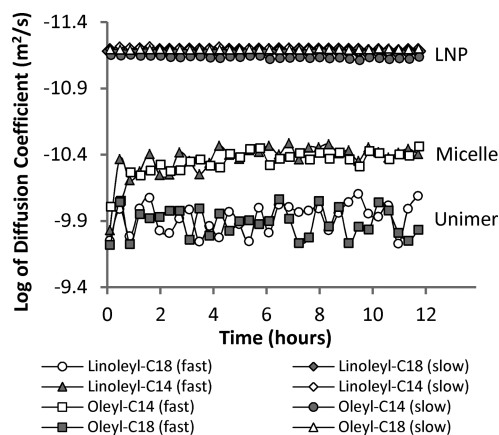


Figure 5. Diffusion coefficients for the LNP associated PEG-lipid and free PEG-lipid collected in rat serum over time. The diffusion coefficients of linoleyl-C14's and oleyl-C14's free PEG-lipid decrease quickly during the first few time points, indicating the formation of micelles.

difficulty in fitting a population that represents ~10% of the population. In addition, the diffusion parameters for the PGSE pulse sequence are not optimized to accurately characterize such a quickly diffusing population. On the other hand, those formulations with a short PEG-lipid tail initially show similar unimer-like diffusion properties, but as more PEG-lipid sheds, the free PEG-lipid population's diffusion coefficient decreases, stabilizing at a more micelle-like value. The resulting micellization indicates that the PEG is not cleaved from its lipid anchor. Micellization of nonionic surfactants require both a hydrophilic and hydrophobic domain. If the PEG-lipid were cleaved in rat serum, then micellization would not be possible, and we have indeed observed that PEG-lipids containing a cleavable linker between lipid and PEG demonstrate a time-dependent transition from micelle-like diffusion to a unimer-like diffusion after contact with serum (data not shown). While all of our measurements with the free PEG-lipids diluted into PBS buffer diffuse stably as micelles over the twelve-hour experiment duration and with a diffusion coefficient identical to that found in serum, it is possible that shed PEG-lipid could anchor into serum lipoparticles, thereby contributing to the population of micelle-like diffusing species. However, our observation of a unimer-like diffusion coefficient rather than a micelle-like diffusion coefficient for the free PEG-lipid population in the serum-containing linoleyl-C18 and oleyl-C18 formulations suggests that lipoprotein association does not occur under the conditions of our experiment.

The stable profiles for the free PEG-lipid of linoleyl-C14 and oleyl-C14 are due to the larger free PEG-lipid populations as well as to their slower diffusion, which is better characterized by the PGSE diffusion settings mentioned in the previous paragraph. For the same reasons, the profiles of the lipid nanoparticle associated PEG-lipids are also stable. This population has diffusion coefficients consistent with DLS measurements. Overall, there are no significant distinctions in diffusion values seen between LNPs composed of the two different cationic lipids.

■ DISCUSSION

We have shown that PGSE NMR provides a new and unique way to study the dynamics of PEG shedding *ex vivo*. Using this method we were able to provide a quantitative and qualitative picture of the PEG shedding phenomenon directly in rat serum. We found that lipid nanoparticles stabilized by PEG-lipids with shorter lipid tails shed more than those with longer lipid tails, in agreement with recent studies by Ambegia⁸ *in vivo* and Xu¹¹ *ex vivo*. Ambegia's impressive report examined PEG-lipid disposition in live mice over a period of 2 h. Radiolabeled PEG-lipid was used to quantify the amount of PEG-lipid eluting with the LNP-containing fraction after chromatographic separation of harvested mouse plasma. The PEG-lipids utilized in their study were of identical structure to ours (the cationic lipids and lipid ratios were different), and for LNPs containing 1.5% of PEG-C-DMA or 1.5% of PEG-C-DSA they found that PEG-lipid shed from the LNP at a rate of >45% per hour and 0.2% per hour, respectively. Ambegia also determined the plasma clearance of the same two LNPs (the LNP concentration was quantified using a radiolabeled and nonexchangeable cationic lipid), finding that the $t_{1/2}$ for the LNPs containing PEG-C-DMA or PEG-C-DSA were 0.64 and 4.03 h, respectively.

Xu examined PEG-lipid shedding *ex vivo* in plasma, using LC/MS–MS to quantify the amount of PEG-lipid eluting with

the LNP-containing fraction after chromatographic separation. The more hydrophobic PEG-lipid utilized in their study was the same as ours (PEG-C-DSA) but the less hydrophobic PEG-lipid was different (C14 lipid tails linked to PEG via ester bonds, “PEG-DMG”). For their LNPs (the cationic lipid was DLinDMA, but the lipid ratios were different from ours) they found that ~50% shed in 15 min for the LNP with 2% PEG-DMG and negligible shedding was observed even after 4 h for the LNP with 2% PEG-C-DSA. Xu also determined the plasma clearance of these two LNPs (the LNP concentration was estimated by measuring the siRNA by RT-PCR, which was assumed to still be encapsulated in an LNP), finding that $t_{1/2}$ for the PEG-DMG and PEG-C-DSA containing LNPs were 0.0519 and 0.832 h, respectively. Overall, the results of Ambegia and Xu indicate a correlation between PEG-shedding rate and plasma clearance of LNPs, and while the correlation is not quantitative, it does suggest that the quantitative determination of PEG shedding can be useful for predicting trends in PEG shedding behavior between similar LNPs.

The simplicity of our approach compared to previously described methods makes it easy to apply to a wide range of particle compositions, and it allows predictions of *in vivo* particle behavior to be made by simple NMR measurements. By this method, the effect of structural variations to the PEG-lipids as well as variations to the particle compositions on the rate of PEG shedding can be assessed without the need for animal experiments or larger scale preparation of formulations. Thus, a wider range of lipid and particle compositions can be explored in biological fluids and species of interest (including humans), allowing for deeper optimization of delivery vehicles and prediction of vehicle behavior.

Extending this method into more biologically relevant conditions is desirable. In particular, using more dilute concentrations of formulation in serum and working at 37 °C would be interesting to study. It is important to emphasize that keeping the ratio of serum to formulation constant is crucial for comparing PEG shedding profiles between LNPs. While not published here, we have seen that changing the ratio of serum to formulation does noticeably affect the shedding rate. Since the dilution upon intravenous injection of LNPs is more severe, and the biological “hosts” for PEG-lipid transfer are more numerous *in vivo*, it is reasonable to expect that PEG-lipid shedding will be more rapid *in vivo* than will be predicted with our method. It is more appropriate to use this method to predict trends (to compare PEG-lipids, to compare LNP compositions, to compare shedding rates in plasma of different species) than establishing absolute *in vivo* PEG-lipid shedding rates.

NMR is notorious for being one of the lower sensitivity analytical techniques, and sensitivity remains a significant limitation of this method. However, the relatively high concentration and fast segmental motion of the analyte (PEG) along with the dilute nature of the medium (rat serum) make this method very transferable to the general study of nanoparticles and polymers, which are commonly PEGylated, in biofluids. It can provide valuable information regarding the dynamics of the system and can potentially be utilized as a screening tool for understanding interactions within the biological milieu. Furthermore, all of this work was performed with a common high resolution NMR probe without any other specialized equipment, making this method of analysis within the grasp of many researchers.

METHODS

Lipid Nanoparticle Preparation and Characterization.

Lipid nanoparticles were prepared by spontaneous mixing through a tee apparatus as previously described.^{18,25,26} Cholesterol and 1,2-distearoyl-*sn*-glycero-3-phosphocholine (DSPC) were purchased from Avanti Polar Lipids (Alabaster, AL) and used as received. The cationic lipids¹⁸ and PEG-lipids²⁷ were racemic and prepared as previously described. The lipids were dissolved in ethanol with the following composition: cationic lipid:cholesterol:1,2-distearoyl-*sn*-glycero-3-phosphocholine:PEG, 40:48:10:2. The siRNA was prepared in 100 mM sodium chloride, 20 mM sodium citrate, and at pH 5 with a 0.9 mg/mL concentration (N/P ratio = 3). The two solutions were then mixed by focusing the streams through the tee with the mixed solution exiting at 90° from the input. The mixed solution was then immediately diluted to 33% ethanol with the citrate buffer. Following a second dilution to 16% ethanol, the lipid nanoparticle solution was concentrated and then diafiltered against PBS by tangential flow filtration. The final solution was sterile filtered (0.2 μm) prior to use. The lipid nanoparticles were monitored for particle size (DLS) on a Malvern ZetaSizer in PBS at room temperature.

¹H PGSE NMR. All NMR measurements were performed on a Bruker AVANCE 400 instrument operating at a basic transmitter frequency of 400.13 MHz. All measurements were acquired using a 5 mm BBFO probe. This probe is capable of a maximum gradient strength of 53 G/cm. Temperature was maintained at 300.0 K with a precision of ±0.1 K. ¹H PGSE NMR diffusion measurements were taken using a pulsed field gradient stimulated echo pulse sequence (Bruker library: steppl1s) as shown in Figure 6.²⁸

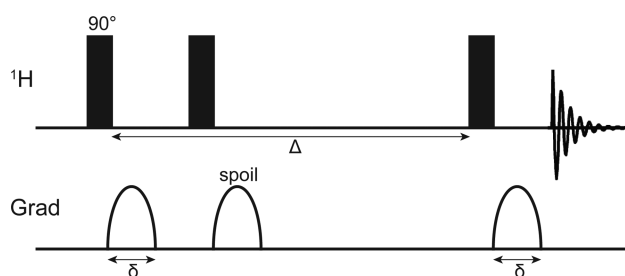


Figure 6. Stimulated echo based PGSE pulse sequence.

Self-diffusion measurements of all LNP samples were performed using 500 μL of formulation. The gradient strength was incremented from 5% to 95% in steps of 16. Diffusion parameters were as follows: a gradient pulse length (δ) of 10 ms, a diffusion time (Δ) of 200 ms, a recycle delay (d1) of 1 s, and an acquisition time of 4 s.

For the PEG shedding analysis, each sample had a total volume of 500 μL. The volume of rat serum (Wistar-Han rat serum, male) was kept constant at 250 μL. 25 μL of D₂O (CIL, 99.96% D) and a variable amount of PBS were used to dilute each formulation to a siRNA concentration of 1.0 mg/mL (PEG-lipid concentration of 1.1 mg/mL) and total volume of 250 μL. The serum and diluted formulation were then briefly vortexed. Time 0 signifies the time at which the serum and LNP formulation were mixed. Necessary probe tuning and matching, shimming, and gain optimization forced the commencement of data acquisition a few minutes after time 0. Acquisition with the deuterium lock on was found to cause distortions about the intense water peak. Subsequently, all

measurements were run with the deuterium lock off to minimize any disturbances. The gradient strength was incremented from 7% to 95% in steps of 16. Diffusion parameters were as follows: a gradient pulse length (δ) of 14 ms, a diffusion time (Δ) of 200 ms, a recycle delay (d1) of 1 s, and an acquisition time of 4 s. Each experiment took roughly 22 min and was repeated in loop for 12 h. A total of 32 points were collected for each formulation.

Theoretical Basis and Data Fitting. The characteristic Stejskal and Tanner equation describes the effect of diffusion time and gradient parameters on signal amplitude as shown in eq 2.²⁹

$$S = S_0 e^{-\gamma^2 \delta^2 g^2 D (\Delta - \frac{\delta}{3})} = S_0 e^{-bD} \quad (2)$$

In this case, *g* is the gradient strength, *S* is the signal amplitude, *S*₀ corresponds to the unattenuated signal intensity at *g* = 0, δ is the gradient pulse width, γ is the gyromagnetic ratio, *D* is the diffusion coefficient, and (Δ − δ/3) is the diffusion time corrected for the effects of finite gradient pulse width. Equation 2 fits a plot of normalized signal intensity versus applied gradient, whereupon the diffusion coefficient of a single species can be obtained.

Determining the diffusion coefficients of two distinct species with overlapping resonances poses a more difficult problem with much literature addressing the issue.^{30,31} However, under certain conditions, the simplest solution is to assume two discrete exponentials and fit the curve to a biexponential decay. Such conditions include high signal-to-noise ratios for both species and a large differential between diffusion coefficients, both of which our system enjoys.³²

$$S = S_{0A} e^{-bD_A} + S_{0B} e^{-bD_B} \quad (3)$$

In eq 3, *D*_A and *D*_B correspond to the diffusion coefficient of each respective species. Relative populations of the two species can be determined by the respective weight factors, *S*_{0A} and *S*_{0B}, with normalization to *S*_{0A} + *S*_{0B}.

All fittings and computation were done in Sigmaplot 11.0 and Microsoft Excel.

AUTHOR INFORMATION

Corresponding Authors

*(C.L.) Novartis Institutes for Biomedical Research, 100 Technology Square, Cambridge, MA 02139. Tel: 617-871-5232. E-mail: cameron.lee@novartis.com.

*(S.R.) E-mail: rajans@gmail.com.

Notes

The authors declare the following competing financial interest(s): All authors were employees of the Novartis Institutes of Biomedical Research during the execution of this research project.

REFERENCES

- (1) Judge, A. D.; Robbins, M.; Tavakoli, I.; Levi, J.; Hu, L.; et al. Confirming the RNAi-mediated mechanism of action of siRNA-based cancer therapeutics in mice. *J. Clin. Invest.* **2009**, *119* (3), 661–673.
- (2) Coelho, T.; Adams, D.; Silva, A.; Lozeron, P.; Hawkins, P.; et al. Safety and efficacy of RNAi therapy for transthyretin amyloidosis. *N. Engl. J. Med.* **2013**, *369* (9), 819–829.
- (3) Whitehead, K. A.; Langer, R.; Anderson, D. G. Knocking down barriers: advances in siRNA delivery. *Nat. Rev. Drug Discovery* **2009**, *8*, 129–138.

- (4) MacLachlan, I. Liposomal formulations for nucleic acid delivery. *Antisense Drug Technology: Principles, Strategies, and Applications*; Crooke, S. T., Ed.; CRC Press: Boca Raton, FL, 2001; pp 237–270.
- (5) Taberero, J.; Shapiro, G. I.; LoRusso, P. M.; Cervantes, A.; Schwartz, G. K.; et al. First-in-humans trial of an RNA interference therapeutic targeting VEGF and KSP in cancer patients with liver involvement. *Cancer Discovery* **2013**, 3 (4), 406–417.
- (6) Fitzgerald, K.; Frank-Kamenetsky, M.; Shulga-Marskaya, S.; Liebow, A.; Bettencourt, B. R.; et al. Effect of an RNA interference drug on the synthesis of proprotein convertase subtilisin/kexin type 9 (PCSK9) and the concentration of serum LDL cholesterol in healthy volunteers: a randomised, single-blind, placebo-controlled phase 1 trial. *Lancet* **2014**, 383 (9911), 60–68.
- (7) Romberg, B.; Hennink, W. E.; Storm, G. Sheddable Coatings for Long-Circulating Nanoparticles. *Pharm. Res.* **2007**, 25 (1), 55–71.
- (8) Ambegia, E.; Ansell, S.; Cullis, P.; Heyes, J.; Palmer, L.; et al. Stabilized plasmid-lipid particles containing PEG-diacylglycerols exhibit extended circulation lifetimes and tumor selective gene expression. *Biochim. Biophys. Acta* **2005**, 1669, 155–163.
- (9) Akinc, A.; Goldberg, M.; Qin, J.; Dorkin, J. R.; Gamba-Vitalo, C.; et al. Development of lipidoid-siRNA formulations for systemic delivery to the liver. *Mol. Ther.* **2009**, 17 (5), 872–879.
- (10) Mui, B. L.; Tam, Y. K.; Jayaraman, M.; Ansell, S. M.; Du, Y. Y. C.; et al. Influence of polyethylene glycol lipid desorption rates on pharmacokinetics and pharmacodynamics of siRNA lipid nanoparticles. *Mol. Ther. Nucleic Acids* **2013**, 2, e139 DOI: 10.1038/mtna.2013.66.
- (11) Xu, Y.; Ou, M.; Keough, E.; Roberts, J.; Koeplinger, K.; et al. Quantitation of physiological and biochemical barriers to siRNA liver delivery via lipid nanoparticle platform. *Mol. Pharmaceutics* **2014**, 11 (5), 1424–1434 DOI: 10.1021/mp400584h.
- (12) Gao, W. G.; Langer, R.; Farokhzad, O. C. Poly(ethylene glycol) with observable shedding. *Angew. Chem., Int. Ed.* **2010**, 49 (37), 6567–6571.
- (13) Price, W. S. Pulsed-field gradient nuclear magnetic resonance as a tool for studying translational diffusion: Part I. Basic Theory. *Concepts Magn. Reson. A* **1998**, 9 (5), 299–336.
- (14) Price, W. S. Pulsed-field gradient nuclear magnetic resonance as a tool for studying translational diffusion: Part II. Experimental Aspects. *Concepts Magn. Reson. A* **1998**, 10 (4), 197–237.
- (15) Momot, K. I.; Kuchel, P. W. Pulsed field gradient nuclear magnetic resonance as a tool for studying drug delivery systems. *Concepts Magn. Reson. A* **2003**, 19A (2), 51–64.
- (16) Occhipinti, P.; Griffiths, P. C. Quantifying diffusion in mucosal systems by pulsed-gradient spin-echo NMR. *Adv. Drug Delivery Rev.* **2008**, 60 (15), 1570–1582.
- (17) Price, W. S. *NMR Studies of Translational Motion: Principles and Applications*; Saykally, R., Zewail, A., King, D., Eds.; Cambridge University Press: New York, 2009; pp 1–68.
- (18) Heyes, J.; Palmer, L. R.; Bremner, K.; MacLachlan, I. Cationic lipid saturation influences intracellular delivery of encapsulated nucleic acids. *J. Controlled Release* **2005**, 107, 276–287.
- (19) Balayssac, S.; Delsuc, M.-A.; Gilard, V.; Prigent, Y.; Malet-Martino, M. Two-dimensional DOSY experiment with excitation sculpting water suppression for the analysis of natural and biological media. *J. Magn. Reson.* **2009**, 196, 78–83.
- (20) Lindman, B. Physico-chemical properties of surfactants. *Handbook of Applied Science and Colloid Chemistry Vol. 1*; Homberg, K., Ed.; John Wiley & Sons: NJ, 2002; pp 421–443.
- (21) Lukyanov, A. N.; Torchilin, V. P. Micelles from lipid derivatives of water-soluble polymers as delivery systems for poorly soluble drugs. *Adv. Drug Delivery Rev.* **2004**, 56, 1273–1289.
- (22) Håkansson, B.; Nydén, M.; Söderman, O. The influence of polymer molecular-weight distributions on pulsed field gradient nuclear magnetic resonance self-diffusion experiments. *Colloid Polym. Sci.* **2000**, 278, 399–405.
- (23) Leal, C.; Rögnvaldsson, S.; Fossheim, S.; Nilssen, E. A.; Topgaard, D. Dynamic and structural aspects of PEGylated liposomes monitored by NMR. *J. Colloid Interface Sci.* **2008**, 325, 485–493.
- (24) Massey, J. B.; Hickon, D.; She, H. S.; Sparrow, J. T.; Via, D. P. Measurement and prediction of the rates of spontaneous transfer of phospholipids between plasma lipoproteins. *Biochim. Biophys. Acta* **1984**, 794, 274–280.
- (25) Hirota, S.; de Ilarduya, C. T.; Barron, L. G.; Szoka, F. C. Simple mixing device to reproducibly prepare cationic lipid-DNA complexes (lipoplexes). *Biotechniques* **1999**, 27, 286–290.
- (26) Jeffs, L. B.; Palmer, L. R.; Ambegia, E. G.; Giebrecht, C.; Ewanick, S.; et al. A scalable, extrusion-free method for efficient liposomal encapsulation of plasmid DNA. *Pharm. Res.* **2005**, 22, 362–372.
- (27) Manoharan, M.; Rajeev, K. G.; Jayaraman, M.; Bulter, D.; Wong, F.; et al. Amino lipid based improved lipid formulation. WO 2009/132131, 2009.
- (28) Tanner, J. E. Use of stimulated echo in NMR diffusion studies. *J. Chem. Phys.* **1970**, 52, 2523–2526.
- (29) Stejskal, E. O.; Tanner, J. E. Spin diffusion measurements: spin echoes in the presence of a time-dependent field gradient. *J. Chem. Phys.* **1965**, 42 (1), 288–292.
- (30) Antalek, B. Using PGSE NMR for chemical mixture analysis: quantitative aspects. *Concepts Magn. Reson. A* **2007**, 30A (5), 219–235.
- (31) Price, W. S. *NMR Studies of Translational Motion: Principles and Applications*; Saykally, R., Zewail, A., King, D., Eds.; Cambridge University Press: New York, 2009; pp 213–214.
- (32) Nilsson, M.; Connell, M. A.; Davis, A. L.; Morris, G. A. Biexponential fitting of diffusion-ordered NMR data: practicalities and limitations. *Anal. Chem.* **2006**, 78, 3040–3045.